Immunity
Article

The Angiogenic Factor PlGF Mediates a Neuroimmune Interaction in the Spleen to Allow the Onset of Hypertension

Daniela Carnevale,[1,2] Fabio Pallante,[1] Valentina Fardella,[1] Stefania Fardella,[1] Roberta Iacobucci,[1] Massimo Federici,[3] Giuseppe Cifelli,[1] Massimiliano De Lucia,[1] and Giuseppe Lembo[1,2,*]
[1]Department of Angiocardioneurology and Translational Medicine, Neuro and Cardiovascular Pathophysiology Research Unit, IRCCS Neuromed, 86077 Pozzilli, Italy
[2]Department of Molecular Medicine, "Sapienza" University of Rome, 00161 Rome, Italy
[3]Department of Systems Medicine, University of Rome "Tor Vergata," 00133 Rome, Italy
*Correspondence: lembo@neuromed.it
http://dx.doi.org/10.1016/j.immuni.2014.11.002

SUMMARY

Hypertension is a health problem affecting over 1 billion people worldwide. How the immune system gets activated under hypertensive stimuli to contribute to blood pressure elevation is a fascinating enigma. Here we showed a splenic role for placental growth factor (PlGF), which accounts for the onset of hypertension, through immune system modulation. PlGF repressed the expression of the protein Timp3 (tissue inhibitor of metalloproteinases 3), through the transcriptional Sirt1-p53 axis. Timp3 repression allowed costimulation of T cells and their deployment toward classical organs involved in hypertension. We showed that the spleen is an essential organ for the development of hypertension through a noradrenergic drive mediated by the celiac ganglion efferent. Overall, we demonstrate that PlGF mediates the neuroimmune interaction in the spleen, organizing a unique and nonredundant response that allows the onset of hypertension.

INTRODUCTION

Hypertension is a leading cause of morbidity and mortality worldwide, being the major risk factor for stroke, heart failure, and kidney diseases (Coffman, 2011; Chobanian, 2009). Although several therapeutic strategies have been developed against the main components involved in blood pressure (BP) homeostasis (i.e., vasculature, kidney, autonomic nervous system), the prevalence of uncontrolled hypertension continues to rise (Lawes et al., 2008) and in the majority of the cases the causes of BP increase are still unknown. Mounting evidence suggests that novel players also contribute to the development of hypertensive disease such as components of the innate and adaptive immune systems (Harrison, 2013; Crowley et al., 2005; Madhur and Harrison, 2012). For example, angiotensin II (AngII), one of the main factors influencing BP levels, has been described as a major trigger of inflammation in several tissues (e.g., resistance vessels and kidney) involved in BP regulation. However, inflammation and immunity have been mostly studied as a part of the injury evoked by hypertension and atherosclerosis (Packard et al., 2009; Kim and Iwao, 2000).

A previous observation showed that mice born with the genetic disease aplasia of the thymus manifest protection in developing hypertension, suggesting the existence of a key role of adaptive immune system (Svendsen, 1976). More recently, an emerging area of investigation revealed that immune cells are crucial players in the onset of hypertension, infiltrating vessel walls and kidneys of hypertensive animals (Bush et al., 2000; Ishibashi et al., 2004; Wenzel et al., 2011) and that mice devoid of lymphocytes also manifest protection in developing AngII-induced hypertension (Guzik et al., 2007). Nevertheless, it is unclear how T cells are activated to contribute to hypertension. Among the manifold inflammatory mediators, placental growth factor (PlGF), belonging to a family of vascular endothelial growth factor (VEGF)-related angiogenic factors, caught our attention given its role of "angiogenic cytokine" and its expression by cells of both the cardiovascular and the immune system (De Falco et al., 2002; Carnevale and Lembo, 2012). Indeed, PlGF participates in pathological angiogenesis in contexts such as tumor environment and wound healing (Luttun et al., 2002; Van de Veire et al., 2010; Bais et al., 2010) and, at the same time, has a specific role in macrophage mobilization (Perelman et al., 2003; Pipp et al., 2003; Carnevale et al., 2011). Moreover, the molecular pathway related to PlGF and sFlt1, a soluble form of its main receptor and its endogenous inhibitor, has been classically associated to pregnancy-related hypertension (Steinberg et al., 2009). Finally, it has also been demonstrated that PlGF is secreted in vascular cells in response to AngII (Pan et al., 2010). Thus, in the present work we aimed to explore the role of PlGF in hypertension. We found that PlGF has a crucial role for the onset of hypertension, played in the splenic immune system. In particular, we unveiled that PlGF mediates a neuroimmune interaction between the sympathetic nervous system and the splenic immune system, which is activated during hypertensive challenges. In the end, we dissected the molecular mechanism regulated by PlGF in the spleen, responsible for the costimulation of T cells, which act as the final effectors in target organs of hypertension.

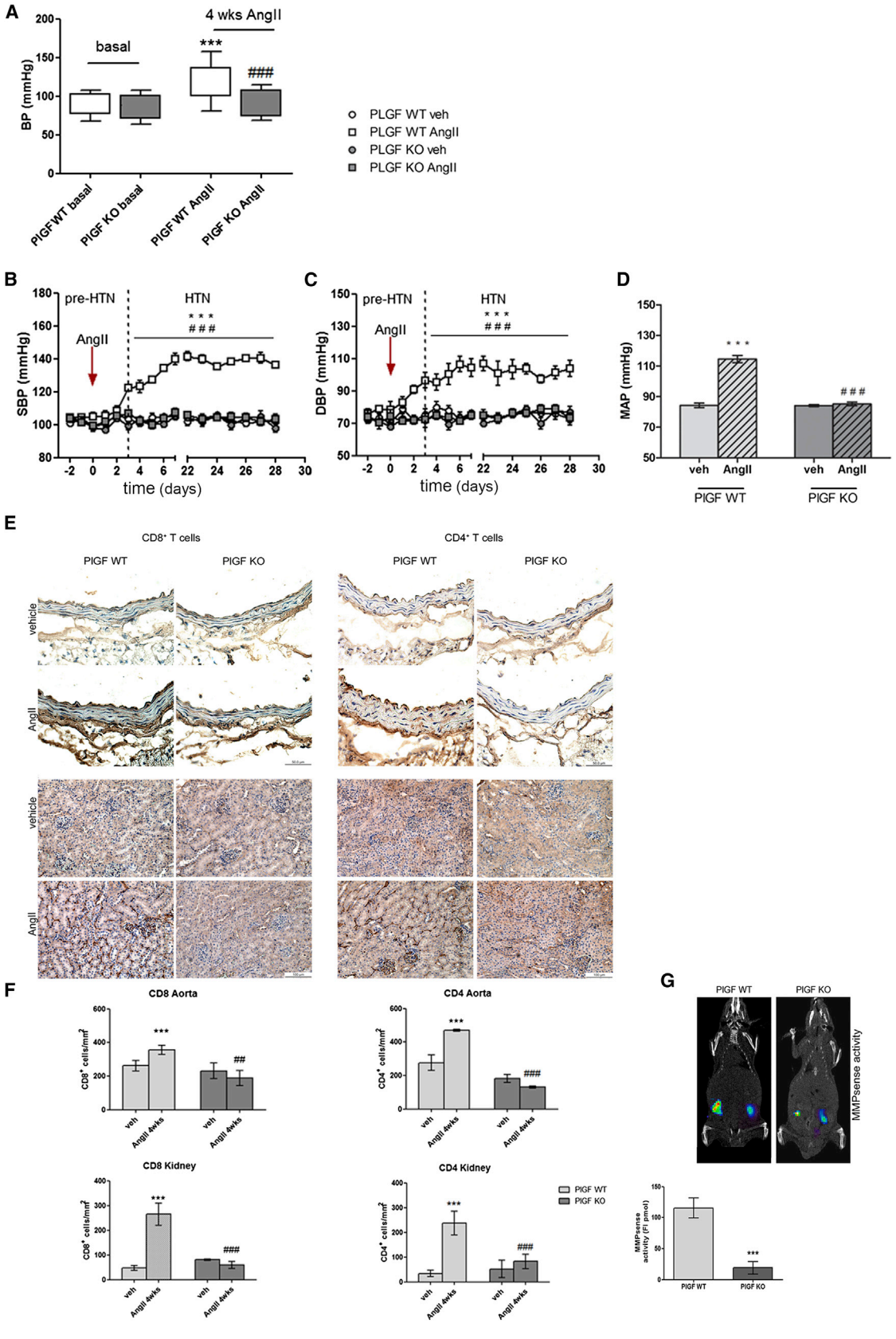

(legend on next page)

RESULTS

Onset of Hypertension Requires PlGF

In WT mice, chronic AngII infusion produced a progressive rise in blood pressure (BP) when measured either by radiotelemetry (Figure 1A) or tail cuff (Figures 1B–1D), becoming significant starting at 4 days after a prehypertensive phase, referred as pre-HTN (Figures 1B–1D). Infusion of vehicle alone had no effect on arterial pressure (Figures 1A–1D). This hypertensive response was completely abolished in mice with genetic deletion of PlGF (encoded by *Pgf*) (Figures 1A–1D). In contrast, the heart rate was similar between wild-type (WT) and PlGF-deficient mice both in basal condition (605 ± 18 versus 634 ± 12 bpm, n.s.) and after chronic AngII (574 ± 22 versus 616 ± 18 bpm, n.s.).

Activation of the renin-angiotensin system through stimulation of type 1 angiotensin receptor is not only a key regulator of BP elevation but also of end-organ damage (Packard et al., 2009; Gurley et al., 2011; Li et al., 2011). Indeed, target organ injury results from both BP-dependent biomechanical challenge and BP-independent hormonal effects. In particular, AngII can directly induce inflammation and fibrosis, thereby contributing to target organ damage. Whereas the echocardiographic analysis after chronic AngII showed the typical cardiac hypertrophic response in WT mice, PlGF-deficient mice were protected from cardiac remodeling (see Table S1 available online). Because chronic kidney disease is also frequently associated with hypertension, we analyzed Masson trichrome and Sirius Red-stained sections of kidney from 4 weeks AngII-infused WT mice, revealing significant fibrosis in both glomeruli and interstitial areas between tubules (Figures S1A and S1B, respectively). In contrast, PlGF-deficient mice were protected from chronic AngII-induced renal damage, as shown by the lack of tissue fibrosis (Figures S1A and S1B). Vascular hypertrophic remodeling has been another recurrent finding in both experimental and clinical hypertension. The AngII-induced increase in wall thickness of thoracic aorta, observed in WT mice, was significantly blunted in the aortas from PlGF-deficient mice (Figure S1C). Finally, hypertension also affects vascular contractile response to agonists. In particular, a higher vasoconstriction was induced by phenylephrine in resistance arteries from WT mice infused with AngII for 4 weeks (Figure S1D). In contrast, resistance arteries isolated from AngII-infused PlGF-deficient mice showed an unaltered response to phenylephrine, comparable to that of vehicle-treated mice (Figure S1D). Thus, these results indicate that the presence of PlGF is required for the typical BP increase to chronic infusion of AngII, given that PlGF-deficient mice show protection from developing hypertension and its related target organ damage.

Immune System Activation to AngII Needs PlGF

In order to investigate the molecular mechanism responsible for the protection from hypertension, observed in PlGF-deficient mice, we first looked for direct vascular effects of the growth factor. In particular, given that we found increased PlGF amounts in vascular tissues (Figure S1E), we stimulated resistance arteries isolated from WT mice with increasing doses of recombinant PlGF, finding no vasoconstricting effect (Figure S1F) but rather a mild vasodilating one (Figure S1F). The same vessels showed typical vasoconstriction and vasodilation when tested with increasing doses of typical agonists, like phenylephrine and acetylcholine, respectively (Figure S1F). To further exclude a direct vascular effect of PlGF in the hypertensive response induced by AngII, we tested the in vivo acute BP responses to increasing doses of AngII, which are typically vasoactive dependent (Figure 1G). Both WT and PlGF-deficient mice showed a comparable increase in systolic (SBP) and diastolic blood pressure (DBP) in the acute response to AngII infused directly in the vasculature (Figure S1G), thus suggesting that the lack of PlGF affects AngII-induced mechanisms during the chronic onset of hypertensive condition.

Considering that PlGF is an "angiogenic cytokine," capable of finely regulating inflammation and immune cells besides its angiogenic effects, we hypothesized that hypertensive stimuli, known to recruit adaptive immune cells, could exploit PlGF to modulate some immune function. It has been demonstrated that activated T cells contribute to vascular remodeling directly on blood vessels via effects of the cytokines produced, or indirectly by actions on the kidney (Harrison et al., 2010). Clearly, chronic AngII infusion induced a marked infiltration of $CD8^+$ and $CD4^+$ T cells in vessels and kidneys of WT mice (Figures 1E and 1F). Conversely, after 4 weeks of AngII infusion, PlGF-deficient vessels and kidneys were devoid of T cell infiltration (Figures 1E and 1F). Moreover, noninvasive fluorescence molecular tomography–CT imaging (FMT-CT) with inflammation-activable sensors (MMPsense), further confirmed the protection from the activation of inflammation or immune system in target organs, as shown by absence of fluorescent pool of probes in kidneys of PlGF-deficient mice after 4 weeks of AngII infusion, as compared to WT (Figure 1G).

To determine whether the protection of PlGF-deficient mice via suppression of T cell infiltration during hypertension had a causal role or was merely a consequence of the lack of BP increase, we analyzed vessels and kidneys early after AngII infusion, in the pre-HTN phase, i.e., at 3 days, before stable BP increase. Although no sign of renal damage was evident in pre-HTN mice, as showed by Masson trichrome and Sirius Red

Figure 1. Onset of Chronic Hypertension and T Cell Vascular Infiltration in Target Organs Induced by AngII Requires PlGF

(A) Telemetric BP monitoring after 4 weeks of AngII in PlGF-deficient mice, indicated herein as PlGF KO (n = 6) versus WT mice (n = 4). Floating bars represent mean ± SEM values of SBP and DBP.

(B–D) Noninvasive tail cuff monitoring of BP response to chronic AngII, in PlGF KO versus WT mice (and respective vehicle infused mice). n = 10 for AngII-treated groups; n = 8 for vehicle-treated groups. Panels represent mean ± SEM values of SBP (B), DBP (C), and MAP (D).

(E and F) Immunostaining and quantitative analysis of CD8 (left panels)- and CD4 (right panels)-positive cells in aortas (upper panels) and kidneys (lower panels) from 4 weeks AngII PlGF KO versus WT mice (and respective vehicle infused mice). n = 6 for AngII-treated groups and n = 4 for vehicle-treated groups. ***p < 0.001 WT-AngII versus WT-veh; ###p < 0.001 PlGF KO-AngII versus WT-AngII (two-way ANOVA followed by Bonferroni's post hoc test).

(G) FMT-CT of in vivo inflammatory activity (MMPsense) in kidneys from 4 weeks AngII PlGF KO versus WT mice. n = 6 for AngII-treated groups and n = 4 for vehicle-treated groups. Fluorochrome concentration is shown in kidneys, on the basis of CT-derived anatomy. Graph showing quantitative analysis of FI (fluorescence intensity) of MMPsense. ***p < 0.001 PlGF KO AngII versus PlGF WT AngII (t test). All data are shown as mean ± SEM.

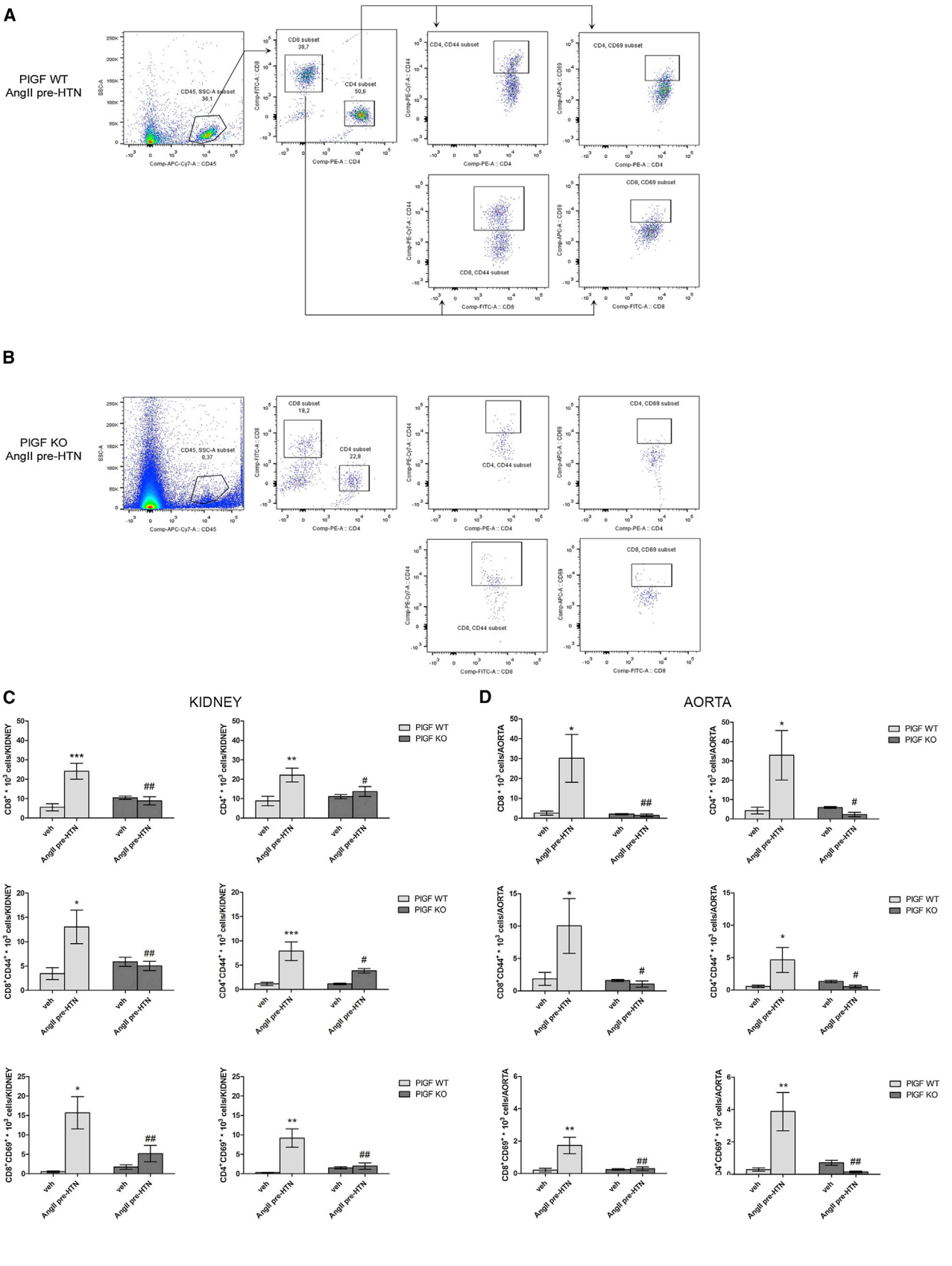

(legend on next page)

stainings on kidney sections (Figures S2A and S2B), $CD8^+$ and $CD4^+$ T cells, positive for the early activation marker CD69 and the homing antigen CD44, were already infiltrated in vessels and kidneys (Figures 2A–2C and Figures S2C–S2H). PlGF-deficient mice showed protection from immune cell infiltration, as compared to pre-HTN WT mice, thus suggesting a mechanistic role of PlGF in immune-system activation during the early development of hypertension. At same time, CD3 cells in the area of splenic white pulp (WP) were increased in pre-HTN AngII PlGF-deficient as compared to WT mice (Figures 3A and 3B), suggesting that the lack of T cell infiltration in target organs could be due to impaired T cells activation and egress from splenic reservoir into circulation toward inflamed target tissues. Thus, concurrent results indicate that, the protection manifested by PlGF-deficient mice in response to AngII induced hypertension, could be ascribed to a role in modulating the splenic immune system more than a more typical vascular action.

A Neuroimmune Interaction Mediates PlGF Release in Hypertension

Lymphocytes homing to target organs during hypertension has been shown to be a crucial step for both raising in BP and end organ damage (Guzik et al., 2007), suggesting that the hypertensive challenge involves innate and adaptive immune responses. In the spleen, the innate and adaptive immune cells are organized to allow rapid sensing of challenges and consequently, molecular interactions that lead to differentiation and migration of T cells (Mueller and Germain, 2009). We found that, besides the vascular production, PlGF is induced in the pre-HTN phase of AngII infusion in the stromal tissue of the spleen along the marginal zone (MZ), as evidenced in the costaining with CD169 and ERTR7, identifying metallophilic marginal zone macrophages and fibroblast reticular cells respectively (Figure 3C and Figures S3A and S3B).

The central nervous system (CNS) plays a pivotal role in AngII-induced hypertension through peripheral sympathetic activation (Marvar et al., 2010). It has been reported that selective removal of sympathetic innervation to the splanchnic district, obtained by celiac ganglionectomy (CGX), markedly attenuated AngII-induced hypertension (King et al., 2007). Considering that the spleen is the splanchnic organ most densely innervated by the sympathetic nervous system (SNS), we hypothesized that the early induction of splenic PlGF upon AngII infusion could be mediated by a neuroimmune interaction. Indeed, amounts of tyrosine hydroxylase (TH), the rate-limiting enzyme for production of noradrenaline (NA) in sympathetic fibers (Dutta et al., 2012; Zigmond and Ben-Ari, 1977), and NA itself, increased in both WT and PlGF-deficient mice in pre-HTN AngII, as evidenced by CD169 and TH double staining (Figure 3D) and quantitative ELISA of NA (Figure S3C). These results were suggestive of a higher sympathetic tone upon AngII challenge, despite the genotype. When we performed CGX in WT mice to look at splenic PlGF we found a marked reduction (Figure 3C and Figures S3A and S3B) thus demonstrating that PlGF is activated by Ang-II induced SNS overactivity. The efficacy of sympathetic splenic denervation obtained with CGX surgery was confirmed by measuring the levels of NA in splenic homogenates (Figure S3C).

In order to provide direct evidence that the sympathetic drive in the spleen is necessary for T cell recruitment into hypertension target organs, we evaluated the presence of infiltrating cells in the aortas and kidneys of CGX mice compared to the sham operated controls, in AngII pre-HTN (Figures S3D and S3E). The sympathetic denervation significantly reduced the number of both $CD4^+$ and $CD8^+$ T cells infiltrating in the aortas (Figure S3D) and in kidneys (Figure S3E) of AngII pre-HTN mice. These results show that at this time the effect is also due to a mechanistic role of splenic nerve and not merely to the lack of BP rising, later observed in this experimental condition. Thus, we highlight a role for PlGF, able to mediate a neuroimmune interaction during hypertensive challenges, being activated by a sympathetic drive, conducted through the celiac ganglion.

Splenic PlGF Is Essential for Hypertension

In order to track unambiguously the fate of T cells from the spleen to the target tissues during hypertension, we studied CD45.2 mice that were splenectomized and given CD45.1 spleens by transplantation and then infused with AngII to induce hypertension. Surgical procedures, control of vitality of transplanted organs, and regrowth of sympathetic innervation are shown in Figures 4A–4D. As shown in Figures 4E and 4F, we observed increased numbers of donor (CD45.1) T cells in aortas and kidneys of AngII pre-HTN animals, demonstrating that the immune cells infiltrating target organs in hypertension are of splenic origin.

Then we sought to identify whether the splenic immune reservoir could be necessary for the establishment of a hypertensive response to AngII. When we challenged splenectomized mice with AngII, they showed a clear protection from BP elevation (Figure 4G) and T cells infiltration (Figures S4A and S4B), demonstrating an essential role of the spleen in hypertension. Interestingly, recent works highlighted the fact that a challenge like myocardial infarction elicits splenic innate immunity, thus suggesting the existence of a pathophysiological link among the cardiovascular and immune system (Swirski et al., 2009).

To define unambiguously the role of PlGF in the onset of hypertension through modulation of the immune system in the splenic reservoir, we studied chimeric mice, generated by spleen

Figure 2. PlGF Is Necessary for Early T Cell Homing after AngII

(A and B) Outline of gating strategy for identification of CD4 and CD8 T cells positive for the early activation marker CD69 and the homing marker CD44 in the aortas. Sample flow-cytometric analyses of single cell suspensions from whole aortas from pre-HTN WT (A) and PlGF-deficient (PlGF KO) mice (B). Gating on leukocytes based on CD45 expression was performed, before analyzing the number of CD4- and CD8-positive cells. Gating on CD45-CD4-positive cells and on CD45-CD8-positive cells was performed to analyze the number of activated cells ($CD69^+$ and $CD44^+$). The same strategy of analysis was applied for T cells isolated from kidney homogenates.

(C and D) Flow cytometric analysis of kidneys and aortas. Quantification shown as absolute numbers of total $CD4^+$ and $CD8^+$ T cells and amount of activated cells marked with CD44 and CD69 antigens. n = 6 per each group. *$p < 0.05$ and **$p < 0.01$ WT-AngII versus WT-veh; #$p < 0.05$ and ##$p < 0.01$ PlGF KO-AngII versus WT-AngII (two-way ANOVA followed by Bonferroni's post hoc test). All data are shown as mean ± SEM.

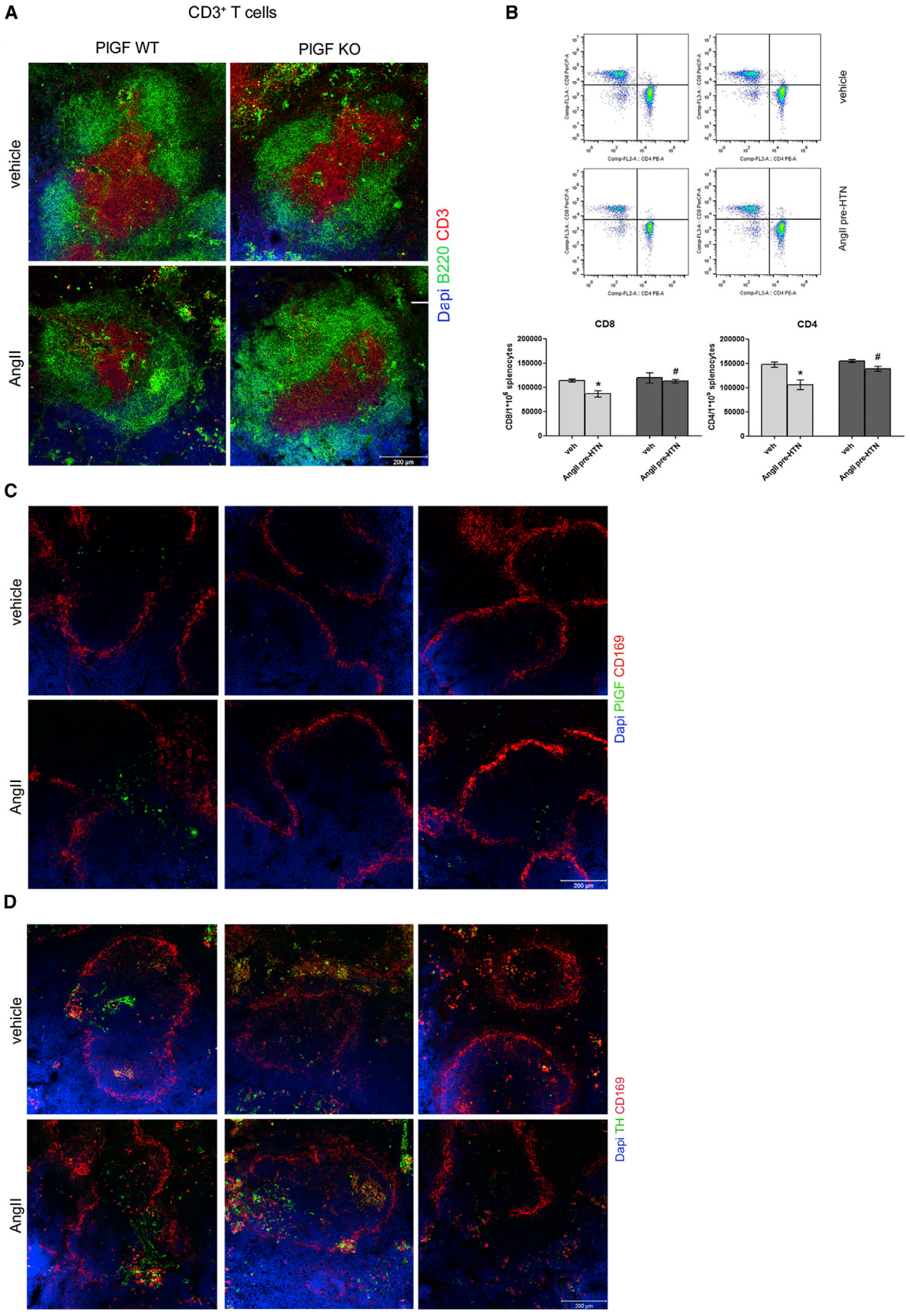

(legend on next page)

transplantation among WT mice and PlGF-deficient mice. Chimeric mice were then subjected to chronic AngII infusion. In WT mice that received PlGF-deficient spleens, AngII failed to raise BP (Figure 4H) and to mobilize T cells into target tissues as shown by the absence of both $CD8^+$ and $CD4^+$ T cell infiltrate (Figures S4C and S4D). When we performed the reverse experiment by transplanting WT spleens into splenectomized PlGF-deficient mice, AngII was able to induce hypertension (Figure 4H) and T cell mobilization into target tissues (Figures S4C and S4D). As a control of these experiments, both WT and PlGF-deficient splenectomized mice received spleens of their same genotype, showing comparable results to nonoperated mice of respective genotypes (Figure 4H and Figures S4C and S4D). Thus, our findings obtained in CD45.1 into CD45.2 chimeric mice show that the spleen is a necessary organ in the development of hypertension, given that T cells homing into target tissues come from the donor spleen. Moreover, at the molecular level, the PlGF-deficient into WT chimeric mice (and vice versa) demonstrate that the expression of PlGF in the spleen is crucial for mobilizing T cells into target tissues and for the onset of hypertension.

PlGF Modulates Timp3 to Check T Cell Costimulation

PlGF is expressed in the MZ of the spleen, in a network of FRCs, identified by the ERTR7 and CD169 antigens (Figure 3C and Figure S3A). This zone of the spleen is particularly enriched in macrophages and dendritic cells with a highly specialized phenotype (Mueller and Germain, 2009) acting as antigen-presenting cells (APCs) and directly or indirectly activating T cells. So far, it is unknown how hypertensive stimuli are able to condition and organize adaptive immune responses in the spleen. Classically this happens when, after antigen uptake, APCs undergo a maturation process characterized by an increased surface expression of major histocompatibility complex II (MHCII) and the B7 ligands, CD80 and CD86 (Song et al., 2008). Interestingly, it has been demonstrated that the AngII hypertensive challenge is able to increase the percentage of cells expressing CD86 in the splenic reservoir, while the number of cells expressing CD80 and MHCII remained unchanged (Vinh et al., 2010). However, how hypertensive stimuli could check the costimulation axis of immune system is unknown.

We found that early upon AngII stimulation, the lack of PlGF significantly protected from CD86 increase in the MZ, as evidenced by the costaining with CD169 (Figure 5A). Flow-cytometry analysis evaluating coexpression of CD86 with CD11b, mainly recognizing monocytes, and CD68-F4/80 for macrophages, in a fraction of monocytes and macrophages enriched from total splenocytes, showed a significant increase of CD86 in macrophages after AngII stimulation (Figures 4B and 4C and Figures S5A and S5B). As evidenced in representative plots and relative quantifications (Figures 4B and 4C and Figures S5A and S5B), the absence of PlGF significantly hampered the expression of CD86 in splenic macrophages, as shown by reduced amount of $CD86^+CD68^+$ cells. These data were further sustained by the reduced expression of $CD86^+$ macrophages localized in CD68 positive area of PlGF-deficient MZ obtained by immunofluorescence (Figure S5C).

We then established a localized gene knockdown experiment of CD86 in the spleen. As shown in Figure 5D, we delivered an antiCD86 siRNA directly into the splenic artery and we evaluated the efficacy of knockdown by flow cytometry (Figures S5D and S5E). Thereafter, we looked at the T cells infiltrating into the target tissues upon AngII infusion, finding a significant reduction of both CD4- and CD8-positive cells (Figures 5E and 5F), thus demonstrating that the activation of splenic CD86 upon AngII challenge is necessary to allow T cells egress.

The modulation of tissue proteins of inflammation is able to condition APCs and consequently activate T cells (Shao et al., 2012). In particular, it has been shown that one of these proteins, the tissue inhibitor of metalloproteinases 3 (Timp3), is a key tissue factor for suppression of costimulation processes (Shao et al., 2012). We have recently found that PlGF has a crucial role in keeping the expression of Timp3 downregulated in cardiac tissue (Carnevale et al., 2011). Thus, we investigated whether the presence of PlGF could be crucial to mediate the crosstalk among innate-adaptive immunity during AngII challenge and depending on costimulation through a checkpoint of Timp3 expression. We found that, while in WT mice AngII did not modify Timp3 expression in the splenic MZ (Figures 6A and 6B), PlGF-deficient mice displayed a strong upregulation of Timp3 expression (Figures 6A and 6B), as evidenced by the colocalization with CD169 and CD68 macrophages. Conversely, no other splenic zones showed this pattern of Timp3 regulation (Figure S6A). To disclose whether the upregulation of Timp3 occurring in absence of PlGF is relevant for hypertension, we used transgenic mice overexpressing Timp3 under the promoter of $CD68^+$ (MacT3 transgenic mice) (Casagrande et al., 2012), inducing Timp3 in splenic macrophages positive for CD169 and CD68 already in basal conditions and further increased by AngII (Figures S6B and S6C). Moreover, we found that the overexpression of Timp3 in $CD68^+$ macrophages hampered the activation of $CD86^+$ in the same $CD68^+$ cells upon AngII infusion, as evidenced by immunofluorescence (Figure 6C) and flow cytometry in a fraction of macrophages enriched from total splenocytes (Figures 6D and 6E and Figures S6D and S6E). When challenged with AngII, MacT3 transgenic mice were protected from development of hypertension (Figure 7A) and T cell

Figure 3. PlGF Is Required for Splenic T Cell Egression and Its Release in the Spleen Is Mediated by a Neuroimmune Interaction

(A) Immunostaining of spleen from pre-HTN PlGF-deficient (indicated as PlGF KO) versus WT mice (and respective vehicle-infused mice), showing $CD3^+$ white pulp (WP), as delineated by counterstaining with B220 antigen recognizing red pulp. n = 6 for AngII-treated groups; n = 4 for vehicle-treated groups.

(B) Flow-cytometry analysis of $CD8^+$ and $CD4^+$ in splenocytes. Plots are representative of n = 6 for group. Quantitative analysis showing absolute T cells labeled with PE and PerCP, respectively and gated on APC-$CD3^+$ cells. n = 6 per group. *$p < 0.05$ WT-AngII versus WT-veh; #$p < 0.05$ PlGF KO-AngII versus WT-AngII (two-way ANOVA followed by Bonferroni's post hoc test). All data are shown as mean ± SEM.

(C) Immunostaining of spleen from pre-HTN PlGF KO versus WT mice (and respective vehicle-infused mice), showing PlGF (green) in the MZ, labeled with anti-CD169 antibody. Images are representative of n = 6 for AngII-treated groups and n = 4 for vehicle-treated groups.

(D) Immunostaining for TH in splenic MZ, showing a comparable increase in PlGF KO and WT mice, after AngII infusion. Selective sympathetic denervation in WT mice, obtained through CGX and documented by the loss of TH staining, hampered the expression of PlGF in the MZ (C).

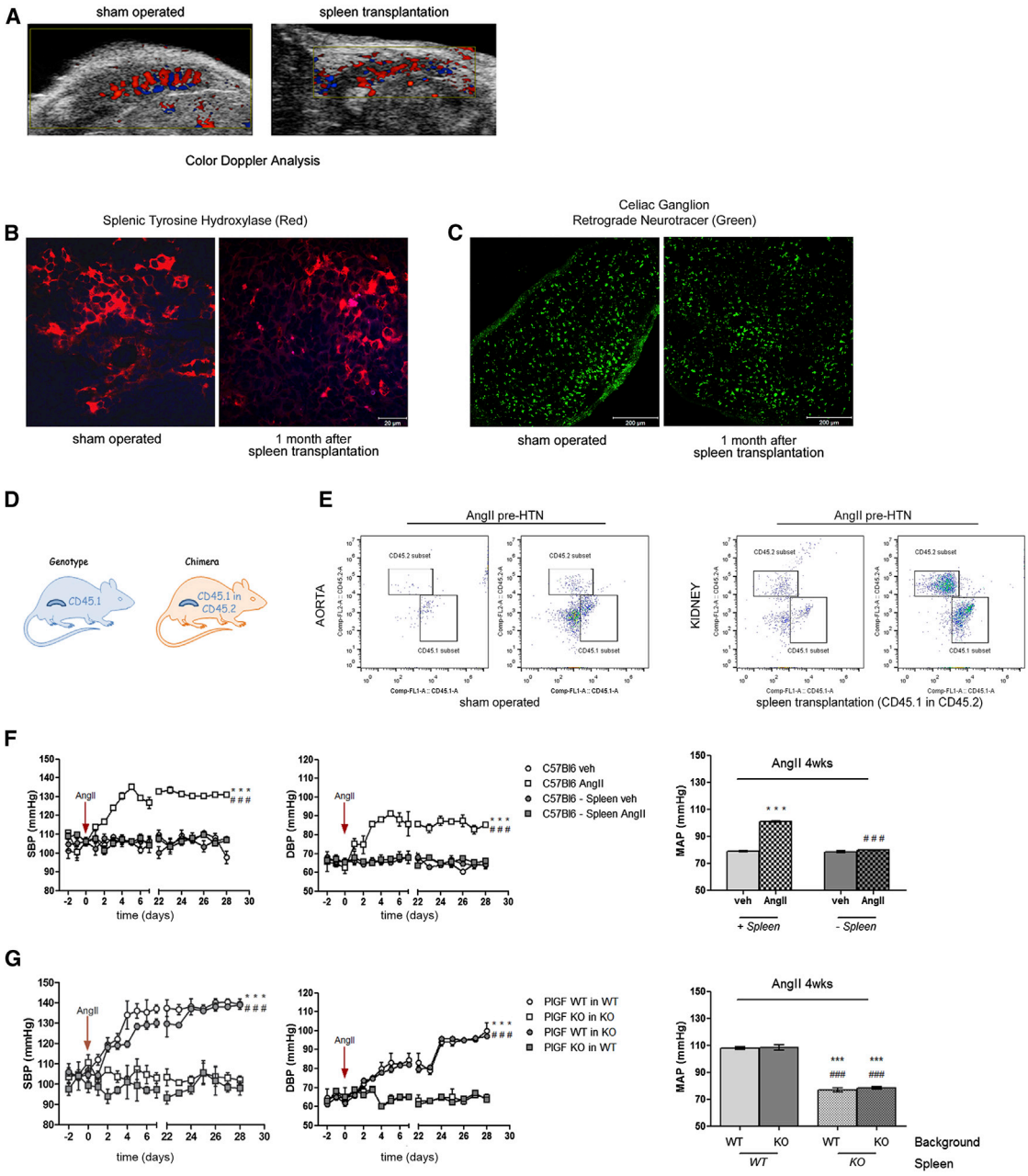

Figure 4. An Essential Role of the Spleen in Hypertension Is Mediated by PlGF

(A) Color Doppler analysis in transplanted spleen and sham operated mice, showing blood vessels within the transplanted or native organ.

(B) TH staining in sections from spleen after 4 weeks from transplantation, documenting regrowth of SNS innervation.

(C) Celiac ganglion neurons labeled with a retrograde fluorescent neurotracer, injected in the splenic parenchyma 4 weeks after spleen transplantation. Celiac ganglions were analyzed 1 week after neurotracer injection.

(D) Cartoon representing chimeric mice obtained after spleen transplantation.

(E) Accumulation of T cells originating exclusively from the donor spleen (CD45.1) as measured by flow cytometry. Dot plots (CD45.1 versus CD45.2) of T cells gated on total leukocytes population in aorta and kidney from AngII pre-HTN mice (sham operated mice are shown as control).

(F) BP response to chronic AngII, in splenectomized WT versus sham mice (and respective vehicle infused mice). n = 6 per group. Panels represent mean ± SEM values of SBP, DBP, and MAP. ***$p < 0.001$ WT AngII versus WT-veh; $^{###}p < 0.001$ WT-AngII-spleen versus WT-AngII (repeated-measures two-way ANOVA followed by Bonferroni's post hoc test).

(G) BP response to chronic AngII, in different groups of chimeric mice, obtained by spleen transplantation among PlGF-deficient (PlGF KO) mice and WT mice. n = 3 per group. Panels represent mean ± SEM values of SBP, DBP, and MAP. ***$p < 0.001$ WT in WT versus KO in KO; $^{###}p < 0.001$ WT in KO versus KO in WT (repeated-measures two-way ANOVA followed by Bonferroni's post hoc test).

infiltration in target organs (Figures S7A–S7F), showing a phenotype matching the one of PlGF-deficient mice. Thus, with these results, we show that PlGF is able to regulate the activation of CD86-dependent costimulation pathway, one of the key mechanisms that are needed for T cells activation. Moreover, we found that this control is exerted through the regulation of Timp3 expression in macrophages.

PlGF Mediates an Epigenetic Checkpoint of Immune System Activation through the Sirt1-p53 Axis

Timp3 is mostly known as a tumor suppressor gene and, as such, it is mainly regulated by transcriptional repression through epigenetic mechanisms not fully understood. Evidence suggests that promoter hypermethylation might not be the predominant epigenetic alteration and that transcriptional repression regulated by p53 might have a predominant role at least in tumors (Loging and Reisman, 1999) where both Timp3 and p53 play crucial roles. Considering that both this pathway and PlGF itself have been classically linked to cancer, we hypothesized that the PlGF-dependent regulation of Timp3 could be related to p53 in hypertension. To clarify this issue, we used a chromatin immunoprecipitation (ChIP) assay to check whether the presence of PlGF is a determinant factor for p53 binding on its element response in Timp3 promoter and its consequent transcriptional repression. While Timp3 is detectable in p53-bound chromatin from WT splenocytes upon AngII, PlGF-deficient splenocytes showed a clear reduction of Timp3 sequence linked to p53 (Figure 7B). Interestingly, the latter is well known to regulate transcription of genes that harbor its response element in the promoter region, depending on its acetylation status (Loging and Reisman, 1999). Because p53 has been identified as a bona fide substrate of Sirt1 deacetylase activity (Vaziri et al., 2001), we looked at Sirt1 in our experimental setting. We found that, in contrast to what observed in WT mice where Sirt1 expression remained unmodified upon AngII, PlGF-deficient mice showed that this deacetylase was significantly increased in the MZ of the spleen (Figure 7C), but not in other splenic districts (Figure S7G). To prove that the control on splenic expression of Timp3, which conditions the milieu necessary for T cells activation and egression in hypertension, is exerted by PlGF through a Sirt1-p53 axis, we performed an in vivo experiment of both pharmacological inhibition and genetic silencing of Sirt1 (Figures 7D and 7E and Figure S7H). PlGF-deficient mice, after both the chronic administration of the selective Sirt1 inhibitor Ex-527 and the genetic knockdown of Sirt1 obtained by local splenic infusion of a Sirt1 siRNA (Figure S7H), allowed restoration of increased BP response to AngII infusion, thus achieving a hypertensive response to levels comparable to that observed in PlGF WT mice (Figures 7D and 7E). With this set of experiments, we have found that PlGF regulates the expression of Timp3, needed as a checkpoint of T cells costimulation in hypertension, through a transcriptional control exerted by the Sirt1-p53 axis.

DISCUSSION

Here we showed an unprecedented role of PlGF in the spleen, orchestrating the immune response to the SNS activated by the hypertensive challenge. Our study brought to light both how important the neuroimmune drive in the spleen is in the genesis of hypertension and, at same time, showed that PlGF is the molecular pathway recruited in the spleen to control BP changes.

Two main findings have guided our study. First, we have found that PlGF-deficient mice manifest protection from AngII-induced hypertension, one of the most common experimental models of hypertension, given that in the human pathology, the use of drugs that target AngII is still one of the main therapeutic approaches used in clinical practice. Second, we have demonstrated an unprecedented and unexpected role of the splenic neuroimmune interaction in hypertension, finding that CGX prevents PlGF induction in the MZ of splenic reservoir upon AngII challenge, and that immune cells infiltrating target organs of hypertension originate from the spleen. Consistent with the latter point, splenectomized mice are protected from AngII-induced BP increase. Strikingly, when we generated chimeric mice by spleen transplantation (PlGF-deficient spleen in WT background and vice versa), we demonstrated that splenic PlGF is indispensable for the onset of hypertension.

We have found that PlGF is crucial to allow T cell costimulation via CD86 and their consequent egress for the deployment toward vasculature of target organs, a hallmark of hypertension. In particular, this effect is exerted by an epigenetic modulation of Timp3 expression, obtained by controlling p53 repressor activity on its promoter that strongly depends on the Sirt1 deacetylase activity.

PlGF has been mainly associated to vascular effects linked to direct vasodilation or to modulation of vascular resistance through binding with the soluble form of its cognate receptor (sFlt1). Thus, our data on the role of PlGF in modulating immunity to establish hypertension would seem at odds with expectations. However, the effects of PlGF on blood pressure regulation described in the present work rely on completely different mechanisms of action. The model of AngII-induced hypertension acutely involves effects that depend on direct regulation of vascular function (where PlGF seems to not to be involved or might even be involved in an opposite way). However, chronic hypertensive pathology induced by AngII infusion is more complex, including the regulation of blood pressure and vascular function, where the immune system plays a crucial role (Guzik et al., 2007). Our data show that PlGF is one of the central molecular players in the chronic phase of the response. On account of this, we reasoned that PlGF has dual effects. On the one hand it has vascular functions that could induce both angiogenic and vasorelaxant effects. On the other hand, PlGF appears as a critical regulator of immune functions, responsible for the activation of T cells in hypertension, a phenomenon well known to be crucial for establishment of chronic hypertension. This could also reconcile the fact that sFlt1, which would lower PlGF availability, has been classically associated to hypertension and principally to preeclampsia.

An important implication of our data is the therapeutic potential. PlGF appears as an appealing molecular target for therapeutic implications because clinical tools to target this pathway already exist (Van de Veire et al., 2010; Bais et al., 2010). In the last years, anti-PlGF monoclonal antibodies have been developed as a strategy to slow tumor growth and for age-related macular degeneration. The ongoing clinical trials testing humanized monoclonal antibodies directed to PlGF provide the

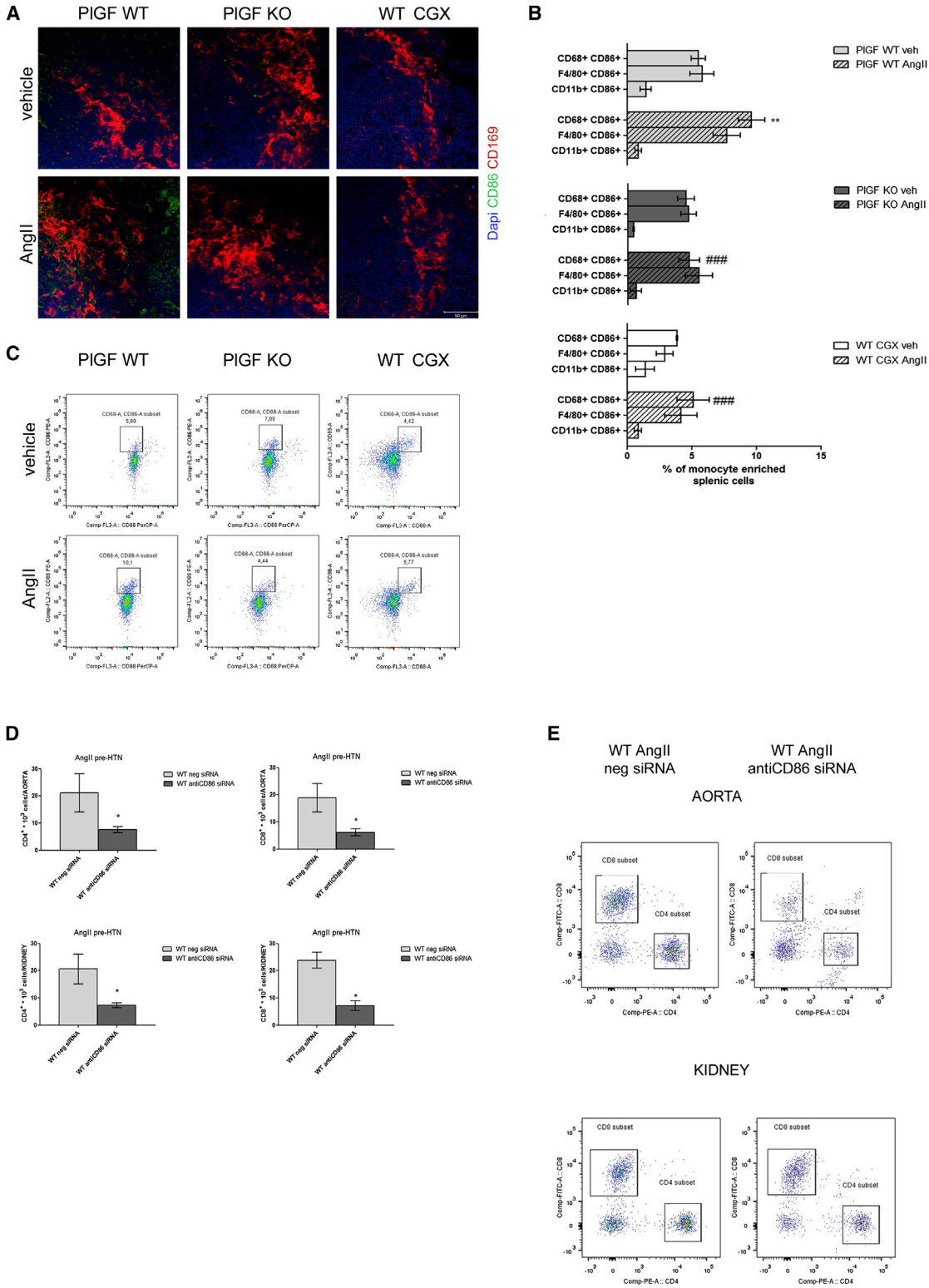

Figure 5. Splenic PlGF Is Required for the Expression of Macrophage CD86 upon AngII, a Crucial Step in the Activation and Egress of T Cells

(A) Immunostaining of spleen from pre-HTN WT mice versus PlGF-deficient (indicated as PlGF KO) and CGX (and respective vehicle infused mice), using anti-CD86 (green) and anti-CD169 (red) antibodies. Images are representative of n = 6 mice per group.

(B and C) Flow cytometric analysis in a fraction of monocytes/macrophages enriched from total splenocytes. Quantitative analysis in (B) showing the percentage of CD86 expression in different fractions of monocytes/macrophages from the enriched population: $CD11b^+$, $F4/80^+$, and $CD68^+$ cells. n = 6 per group. $^{**}p < 0.01$

(legend continued on next page)

possibility to target it in hypertension too. There is a pressing need for new treatments to reach satisfactory control rates in the substantial proportion of people with hypertension who do not achieve the BP target levels recommended by current guidelines. At same time, our findings raise an intriguing question about the effect of PlGF inhibition in cancer, concerning its dependence on the previously unknown capability to exert an epigenetic modulation of p53-Timp3 axis, which is well known to play a crucial role also in tumor growth.

EXPERIMENTAL PROCEDURES

Animals

All animal handling and experimental procedures were performed according to European Communities guidelines (EC Council Directive 2010/63) and the Italian legislation on animal experimentation (Decreto L.vo 116/92). The protocol was approved by the Italian Ministry of Health (Permit number 58/2012-B). Mice of 12–15 weeks were used in all experiments. PlGF-deficient mice were backcrossed for 11 generations in C57Bl/6J mice from the original strain in 50% 129Sv/ 50% Swiss mice (Gigante et al., 2006). MacT3 transgenic mice were generated as described elsewhere and backcrossed with C57Bl/6J (Casagrande et al., 2012). WT mice with the same genetic background (C57Bl6/J) served as control in both cases. B6.SJL-PtprcaPep3b/BoyJ (CD45.1$^+$) were used for spleen transplantation experiments.

According to our experience and current literature on the same experimental models (Guzik et al., 2007; Swirski et al., 2009; Vinh et al., 2010; Wenzel et al., 2011; Carnevale et al., 2012), the number of animals in each setting used was enough to determine whether there was a significant difference among groups, as tested by the software PS3.0

Angiotensin II (0.5 mg/kg/day) or vehicle (NaCl 0.9%) were delivered subcutaneously with osmotic minipumps (model 1007D, ALZET). At day 3 or 28, accordingly to experimental design, mice were euthanized by overdose of sodium pentobarbital anesthesia.

Celiac Ganglionectomy

In mice anesthetized with ketamine-xylazine, the celiac ganglion area was exposed through a midline laparotomy. Aorta and celiac artery were isolated and the ganglion was removed. For sham mice, the ganglion area was exposed and aorta and celiac artery were isolated, without removing the ganglion.

Splenectomy

Under isoflurane anesthesia (2–5 Vol%), supplemented with 1 L/min oxygen, the abdominal cavity of mice was opened and splenic vessels were cauterized. The spleen was carefully removed. For control experiments, the abdomen was opened as well, without spleen removal.

Generation of Chimeric Mice by Spleen Transplantation

The surgical procedure for spleen transplant was performed with some modifications, accordingly to the methodology of Swirski and colleagues (Swirski et al., 2009). Briefly, donor mice were anesthetized with an intraperitoneal injection of ketamine (90 mg/kg) and xylazine (10 mg/kg), followed by an intravenous injection of heparin (Hospira). A longitudinal incision in the abdomen of the donor allowed to the spleen. The aortic cuff connected to the splenic artery, allowed vascular anastomosis of the spleen to the recipient. The recipient mouse was anesthetized with isoflurane (2-5 Vol%) supplemented with 1 L/min oxygen. An abdominal midline incision was made to visualize the spleen and vasculature. After isolation, the recipient splenic artery and vein were clamped, then anastomosis among donor and recipient splenic veins and arteries were created using 10.0 suture (Premilene, Braun) and clamp was then removed to restore blood flow. Mice were allowed to recover for at least 4 weeks and a fully restoration of blood supply, tissue oxygenation, and regrowth of sympathetic nervous system innervation were controlled.

siRNA Injection

In mice anesthetized with ketamine-xylazine, after isolation of the splenic artery and insertion of a micro medical tubing, Ambion In Vivo Pre-designed siRNA Sirt1 (s96766) and siRNA CD86 (s63710) complexed with Invivofectamine 2.0 Reagent (18.75 nmol/dose) was delivered with a syringe pump (WPI) at a constant infusion velocity. Control mice received an equal amount of a siRNA targeted to luciferase (Sigma Aldrich) and Ambion In Vivo Neg Control #1 siRNA, complexed with Invivofectamine 2.0 Reagent and delivered with the same procedure. Mice received AngII (0.5 mg/kg/day) with osmotic minipumps, at day 3 after siRNA delivery.

Blood-Pressure Measurements

Arterial blood pressure was monitored telemetrically, as previously described (Brancaccio et al., 2003) by the HD–X11 pressure transmitters (Data Sciences International) implanted in anesthetized mice with ketamine/xylazine. Radio signals from the implanted transmitter were captured by the Physiotel RPC-1 receiver (Data Sciences International), and the data were stored online using the Dataquest Ponemah 4.9 acquisition system (Data Sciences International).

Conventional Blood Pressure Monitoring Was Held in Conscious Mice with Tail-Cuff Plethysmography

In vivo acute pressure response study to AngII was conducted in anesthetized mice with isoflurane. An arterial catheter was connected to a pressure transducer, MPVS ultra (Millar), and a venous catheter was used for drug injection. Bolus injections of increasing doses of AngII (1–100 μg/kg) were administered at least 2 min intervals. Dose response curves were established for the peak of the BP responses.

Ultrasound Imaging

Ultrasound analysis was performed in mice anesthetized with tribromoethanol (175 mg/kg), using Vevo 2100 device equipped with 18–38 MHz linear-array transducer with a digital ultrasound system (Visualsonics), as previously described (Carnevale et al., 2011).

Fluorescence Molecular Tomography–Computed Tomography Imaging

Mice anesthetized with ketamine/xylazine were immobilized in a multimodal-imaging cartridge, provided with fiducial marks on the frame that enable, after acquisition of multiple imaging, the exact fusion of images with microCT. A commercially available FMT system was used for in vivo imaging studies (FMT1500, Perkin Elmer). 2 nmol per mouse of MMPsense 680 (Perkin Elmer) were injected intravenously. Data were postprocessed using True Quant software (Perkin Elmer) and FMT/CT DICOM images were fused with Amide Medical Imaging Data Examiner Software, using fiducial points to define X-Y-Z coordinates for both data sets.

Vascular Function Evaluation

Second-order mesenteric arteries were dissected out from anesthetized mice and set up on wire myograph (DMT Instruments), in gassed KREBS, pH 7.4, at 37°C, under a normalized tension corresponding to an effective pressure of 75 mmHg. Concentration-response curves were performed for PlGF and phenylephrine and, then, with PlGF and ACh in vessels precontracted with phenylephrine at 80% of KPSS contraction. All substances used were from Sigma, except recombinant PlGF that was from R&D Systems.

ELISA for Determination of PlGF

PlGF levels were measured in triplicate for each sample, extracted with a buffer containing PBS and protease inhibitor cocktail (Sigma), by a high

versus WT-veh; $^{###}p < 0.001$ versus WT-AngII (two-way ANOVA followed by Bonferroni's post hoc test). Data are mean ± SEM. Representative plots in (C), showing PE-labeled CD86$^+$ cells colocalize with PerCP-labeled CD68$^+$ cells (gated on total cells from the enriched population).
(D and E) Intrasplenic siRNA delivery for CD86 knocking down in WT mice. (D) Intrasplenic knockdown of CD86 in WT mice hampered the early T cells homing in aortas and kidneys after AngII infusion. n = 4 per group. $^*p < 0.05$ versus WT-AngII neg siRNA (unpaired t test). All data are shown as mean ± SEM.

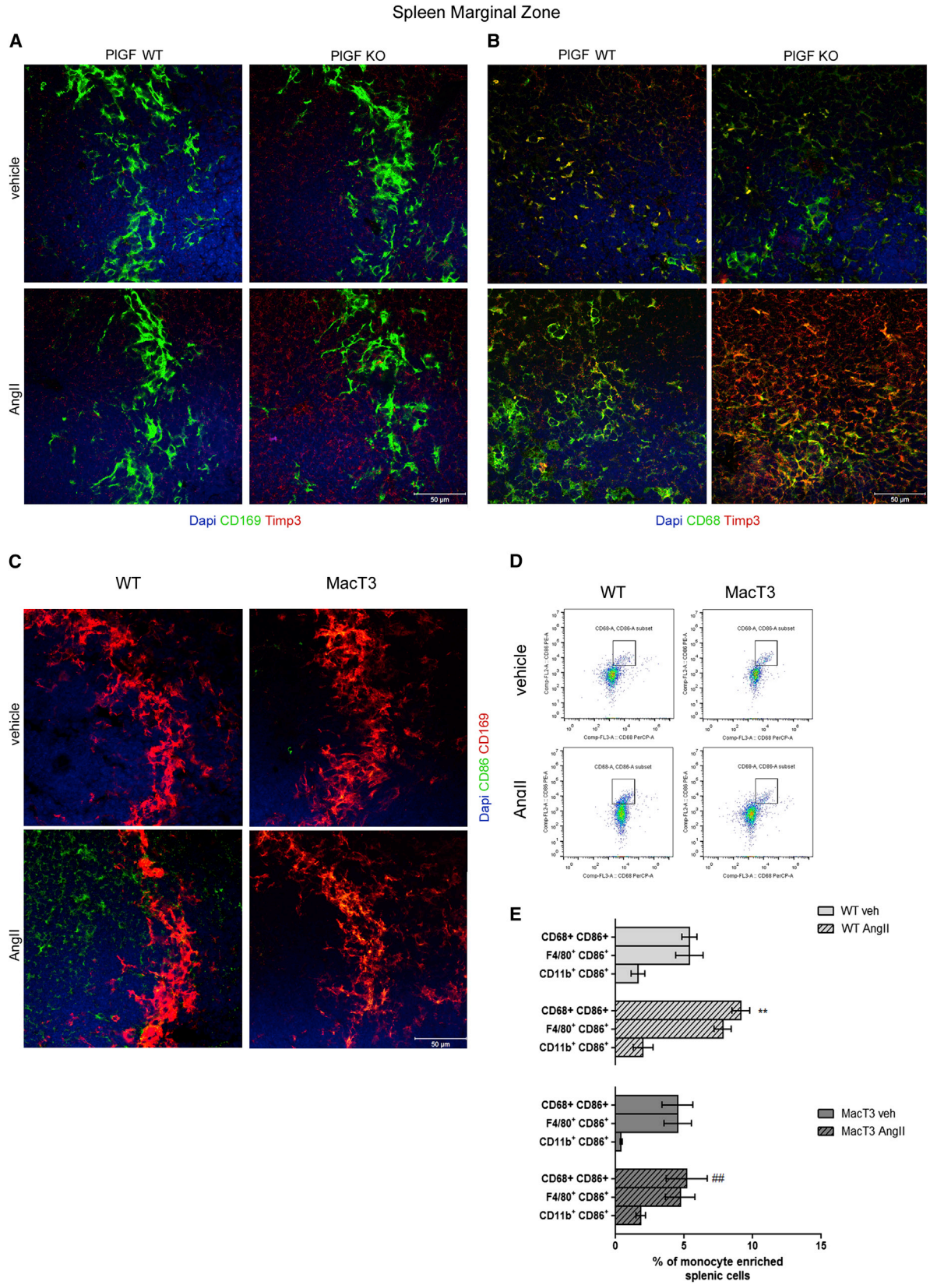

(legend on next page)

sensitivity ELISA kit (R&D Systems), following manufacturer's instructions. Results are expressed as pg/mg of total proteins, as measured by Bradford Assay kit (Biorad).

ELISA for Determination of Noradrenalin

Noradrenalin levels were measured in duplicate for each sample, extracted with a buffer containing 0.1N HCl and 1mM EDTA, by a high sensitivity ELISA kit (IBL International), following manufacturer's instructions. Results are expressed as pg/g of weight tissue.

Isolation and Preparation of Single Cell Suspensions from Spleen, Kidney and Aorta

Mice were anesthetized with ketamine/xylazine and spleen was isolated. Then, mice were exsanguinated and both kidneys and aorta were collected. Spleen was mechanically disrupted and then passed through a 40 μm sterile filter (Falcon, BD) and centrifuged at 300× g for 10 min. After a treatment with ACK Lysing Buffer (Lonza), the pellet was resuspended in PBS. Total splenic leukocytes were stained and analyzed using flow cytometry or used to isolate and enrich monocytes/macrophages by negative selection, using a commercially available monocyte enrichment kit (EasySep Kit and Purple EasySep Magnet, Stemcell Tech).

Kidney cell suspension was obtained disrupting mechanically two decapsulated kidneys, and then passed through a 70 μm sterile filter (Falcon, BD). The resulted cell suspension was centrifuged at 300× g for 10 min. To isolate lymphocytes from cell suspension, the pellet was then suspended in 36% Percoll (Sigma), gently overlaid onto 72% Percoll, and centrifuged at 1,000× g for 30 min at RT.

Aorta cell suspension was obtained disrupting mechanically the tissue and digesting the suspension in Digestion Cocktail, was then passed through a 70 μm sterile filter (Falcon, BD), and centrifuged at 300× g for 5 min to pellet the cells.

Before proceeding with stainings for flow-cytometric analyses, lymphocytes from kidney and aorta total cells were enriched with Mouse T Lymphocyte Enrichment Set-DM (BD IMag).

Samples were resuspended in PBS and then the number of the cells was assessed using trypan blue and an automated counter (Countess, Life Technologies).

Flow Cytometry Analysis

Splenic leukocytes (1×10^6), enriched monocytes (2×10^5), total kidney, and aorta lymphocytes were preincubated with anti-CD16/32 Fc receptor and then incubated with various combinations of mAbs, washed with PBS, centrifuged at 300× g for 5 min at 4°C, and resuspended in FACS buffer. Immunofluorescence staining was analyzed using a C6 Accuri Flow Cytometer and BD FACSCanto (BD Biosciences). The data were analyzed using FlowJo Software.

Antibodies

The fluorochrome-conjugated mAbs to mouse antigens used for flow cytometry analysis were as follows: anti-CD16/CD32 (2.4G2), PE anti-CD86 (GL1), PE Isotype control Rat IgG2a, APC anti-CD11b (M1/70), PerCP-Cy5.5 anti-CD8a (53-6.7), FITC anti-CD8a (53-6.7), APC anti-CD3e (145-2C11), PerCP anti-CD45 (30-F11), FITC anti-CD4 (RM4-5), PE anti-CD4(RM4-5), APC anti-CD69 (H1.2F3), APC-Cy7 anti-CD45 (30-F11), PE-Cy7 anti-CD44 (IM7) (BD PharMingen), FITC anti-F4/80 (FA-11) (AbD Serotec), and PerCP-Cy5.5 anti-CD68 (FA-11) (BioLegend).

Chromatin Immunoprecipitation

Total splenocytes (2×10^7) were analyzed using Enzymatic Chromatin IP Kit (Agarose Beads), as detailed by manufacturer's instructions (Cell Signaling). Briefly, anti-p53 1:500 antibody (Cell Signaling) was used for ChIP (10 μg of crosslinked chromatin). The amount of Timp3 gene in the p53-immunoprecipitated chromatin was detected by PCR (Eppendorf Mastercycler) and normalized with the total amount of the gene present in the 2% input of chromatin of each immunoprecipitated sample.

Immunoblot

Splenocyte proteins were extracted with lysis buffer 1X (Cell Signaling) plus 1 mM phenylmethylsulfonyl fluoride (Sigma) and centrifuged at 14,000× g for 20 min. Total proteins were determined with Pierce BCA Protein Assay Kit (Thermo Scientific). Proteins were resolved by SDS-PAGE followed by immunoblotting using the following antibodies: rabbit anti-Sirt 1:500 (Millipore), mouse anti-Gapdh 1:1000 (Santa Cruz). Secondary antibodies used were: donkey anti-rabbit (1:5000) and goat anti-mouse (1:5000), from Santa Cruz. Protein detection was performed with ECL kit (Amersham) and densitometry was obtained with the Quantity One 1-D Analysis Software.

Histological Analysis, Immunohistochemistry, and Immunofluorescence

Haematoxylin–eosin (H&E), Masson's trichrome, and Picrosirius Red stainings were performed according to standard procedures. Sections of kidney were deparaffinized, rehydrated, and then underwent antigen retrieval. Vessels were embedded in OCT (Leica Microsystems), postfixed with 4% paraformaldehyde for 15 min. Slides were processed for immunohistochemistry with the following primary antibodies: anti-CD8 and anti-CD4 (1:50; BD PharMingen). Appropriate biotinylated secondary antibodies (1:200; Vector) were used for successive processing with DAB (Vector). Hematoxylin (Sigma) was used as counterstaining. The number of CD8 and CD8-positive cells per mm^2 was determined using the Image J software Cell Counter plugin analysis tool.

For immunofluorescence analysis, 25 μm sections from spleen were postfixed with 4% paraformaldehyde for 15 min and processed for staining with the following primary antibodies: rabbit anti-Timp3 (Novus biologicals) 1:500, rabbit anti-PlGF (Abcam) 1:250, rabbit-anti CD86 (Novus Biologicals) 1:100, rat anti-mouse CD68 (AbD Serotec) 1:200, rat anti mouse CD169 (AbD Serotec) 1:100, Sheep-anti Tyrosine Hydroxylase (Millipore) 1:800, rat anti-mouse CD45R (B220, BD PharMingen) 1:50, anti-hamster CD3 (BD PharMingen) 1:50, Rabbit anti-Sirt1 (Millipore) 1:250, and rat anti-ER-TR7 (Acris) 1:200. Sections were then incubated with the respective secondary antibodies conjugated to Alexa Fluor 488, Alexa Fluor 647 or Cy3. Slides were then coverslipped with DAPI containing medium (Vector). 25 μm sections were obtained with cryostat microtome by celiac ganglion retrogradely labeled with Hydroxystilbamidine methanesulfonate injected in the spleen and mounted and coverslipped for analysis.

Confocal Microscopy Analysis

All coverslipped mounted tissue sections were scanned using a Zeiss 780 confocal laser scanning microscope with a Zeiss ECPLAN-NEOFLUAR 10x/0.30 M27, ECPLAN-NEOFLUAR 20x/0.50 M27, ECPLAN-NEOFLUAR 40×/1.30 M27 oil immersion objective or PLAN-APOCHROMAT 63×/1.4 oil DIC oil immersion objective (Carl Zeiss Microimaging Inc.). We used a 405 Diode laser to excite DAPI, a 488 nm argon laser to excite Alexa Fluor 488, and a 543 HeNe laser to excite Cy3. Pseudocoloring was performed using ZEN software (Carl Zeiss Microimaging).

Figure 6. PlGF Repression of Macrophage Timp3 Is Crucial for AngII Induction of CD86 and Hypertensive Response

(A and B) Immunostaining of spleen from pre-HTN PlGF-deficient (indicated as PlGF KO) and WT mice (and respective vehicle infused mice), showing Timp3 expression in $CD68^+$ MZ macrophages, using anti-CD169 (A) and anti-CD68 (B) antibodies. Images are representative of n = 6 experiments.

(C) Immunostaining of spleen from pre-HTN MacT3 mice (and vehicle infused mice) as compared to WT mice, using anti-CD86 (green) and anti-CD169 (red) antibodies. Images are representative of n = 6 mice per group.

(D) Representative flow cytometric analyses in a fraction of monocytes/macrophages enriched from total splenocytes. PE-labeled $CD86^+$ cells colocalize with PerCP-labeled $CD68^+$ cells from pre-HTN MacT3 versus WT mice (gated on total cells from the enriched population).

(E) Quantitative analysis showing percentage of CD86 expression in different fractions of monocytes/macrophages from the enriched population: $CD11b^+$, $F4/80^+$, and $CD68^+$ cells. n = 6 per group. $^{**}p < 0.01$ and $^{***}p < 0.001$ WT-AngII versus WT-veh; $^{\#\#}p < 0.01$ and $^{\#\#\#}p < 0.001$ MacT3 transgenic-AngII versus WT-AngII (repeated-measures two-way ANOVA followed by Bonferroni's post hoc test). Data are mean ± SEM.

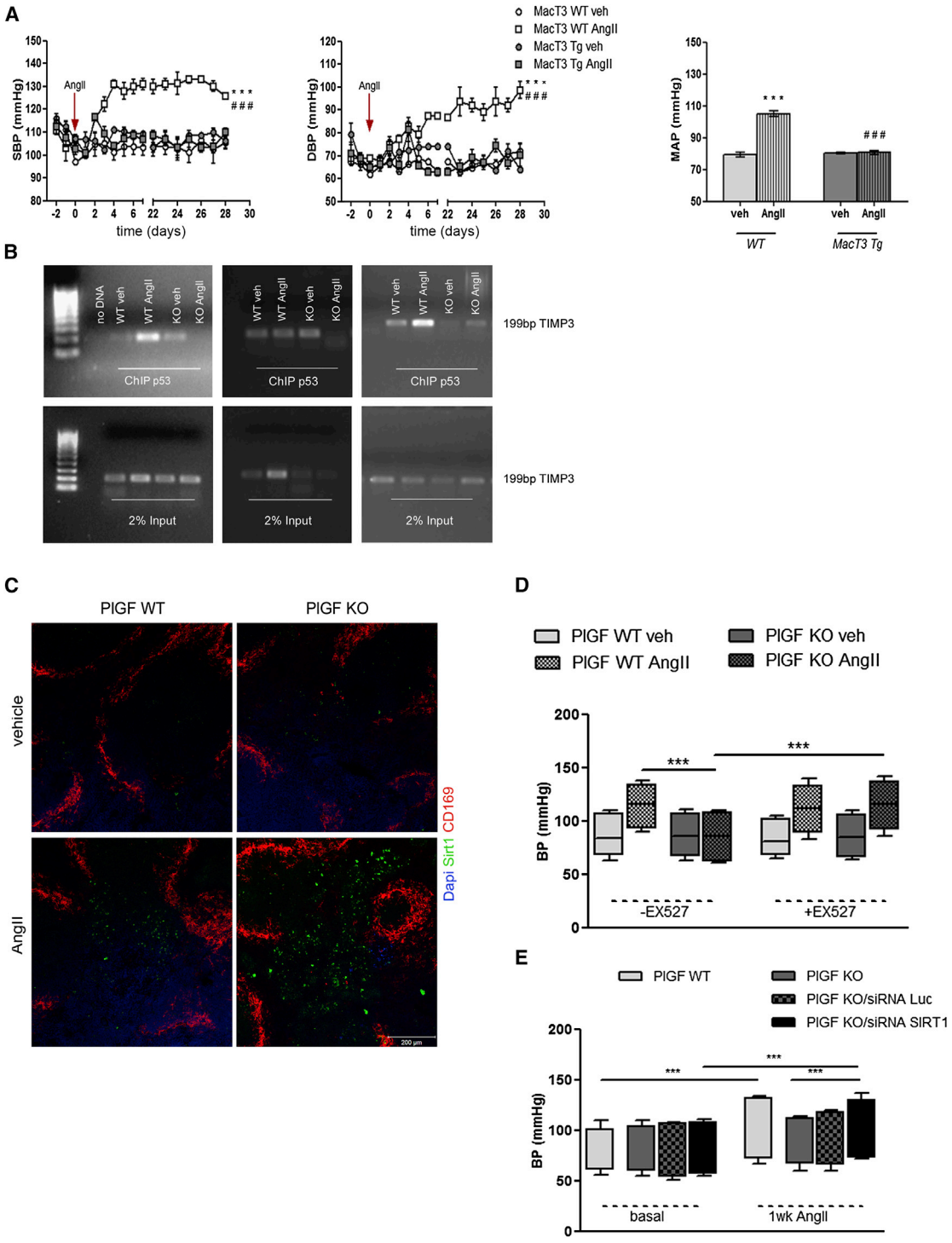

Figure 7. PlGF Exploits an Epigenetic Mechanism to Exert a Checkpoint of Immune System Activation in Hypertension

(A) BP response to chronic AngII in MacT3 transgenic and WT mice (and respective vehicle infused mice). n = 6 for AngII-treated groups and n = 4 for vehicle-treated groups. Panels represent mean ± SEM values of SBP (left), DBP (middle), and MAP (right).

(B) Timp3 PCR in p53 ChIP (upper panels) and respective 2% input (lower panels) of chromatin of splenocytes from AngII-infused PlGF-deficient (indicated as PlGF KO) and WT mice (and respective vehicle-infused mice). Images represent three independent experiments for each experimental group.

(C) Immunostaining showing Sirt1 (green) expression in splenic MZ, evidenced by CD169 staining (red), in AngII-infused PlGF KO and WT mice (and respective vehicle-treated mice).

(D and E) BP response to chronic AngII, in PlGF KO mice treated with Sirt1 selective pharmacological inhibitor EX-527 (D) and genetic inhibition of splenic Sirt1 obtained by local in vivo infusion of a Sirt1 siRNA (E), as compared to a luciferase-targeted siRNA.

Bright-field Microscopy Analysis

All images were captured using a DMI3000B Leica optical microscope provided of Leica cameras (Leica Microsystems) and processed with the Leica Application Suite (LAS V3.3).

Statistical Analysis

Data are presented as mean ± SEM. Statistical significance was calculated accordingly to the experimental design, as indicated in the figure legends. $p < 0.05$ was considered significant. Statistical analyses were performed with GraphPad software PRISM5 (GraphPad Software).

SUPPLEMENTAL INFORMATION

Supplemental Information includes seven figures, one table, and Supplemental Experimental Procedures and can be found with this article online at http://dx.doi.org/10.1016/j.immuni.2014.11.002.

AUTHOR CONTRIBUTIONS

D.C. conceived the research, supervised experiments, analyzed data, performed statistical analysis, drafted the manuscript, and handled funding. F.P. and V.F. performed microsurgery and models of hypertension, measured invasive blood pressure, and performed in vivo FMT/CT in vivo imaging. S.F. and R.I. performed molecular and histological analysis. R.I. performed flow cytometry analysis. M.F. provided MacT3 transgenic mice. G.C. performed ultrasound imaging. M.D.L. and V.F. provided animal handling. M.D.L. performed noninvasive BP monitoring. G.L. conceived the research, interpreted data, handled funding, supervised the research, and drafted the manuscript.

ACKNOWLEDGMENTS

This work was supported by the following grants: PON01_00829 and PON01_01227 by MIUR (Italian Ministry of University and Research) to G.L.; ''Ricerca corrente'' by MOH (Italian Ministry of Health) to G.L.; research grant from SIIA (Italian Society of Hypertension) to G.L.; and Pasteur Institute - Fondazione Cenci Bolognetti to D.C.

Received: May 20, 2014
Accepted: September 23, 2014
Published: November 20, 2014

REFERENCES

Bais, C., Wu, X., Yao, J., Yang, S., Crawford, Y., McCutcheon, K., Tan, C., Kolumam, G., Vernes, J.M., Eastham-Anderson, J., et al. (2010). PlGF blockade does not inhibit angiogenesis during primary tumor growth. Cell *141*, 166–177.

Brancaccio, M., Fratta, L., Notte, A., Hirsch, E., Poulet, R., Guazzone, S., De Acetis, M., Vecchione, C., Marino, G., Altruda, F., et al. (2003). Melusin, a muscle-specific integrin beta1-interacting protein, is required to prevent cardiac failure in response to chronic pressure overload. Nat. Med. *9*, 68–75.

Bush, E., Maeda, N., Kuziel, W.A., Dawson, T.C., Wilcox, J.N., DeLeon, H., and Taylor, W.R. (2000). CC chemokine receptor 2 is required for macrophage infiltration and vascular hypertrophy in angiotensin II-induced hypertension. Hypertension *36*, 360–363.

Carnevale, D., and Lembo, G. (2012). Placental growth factor and cardiac inflammation. Trends Cardiovasc. Med. *22*, 209–212.

Carnevale, D., Cifelli, G., Mascio, G., Madonna, M., Sbroggiò, M., Perrino, C., Persico, M.G., Frati, G., and Lembo, G. (2011). Placental growth factor regulates cardiac inflammation through the tissue inhibitor of metalloproteinases-3/tumor necrosis factor-α-converting enzyme axis: crucial role for adaptive cardiac remodeling during cardiac pressure overload. Circulation *124*, 1337–1350.

Carnevale, D., Vecchione, C., Mascio, G., Esposito, G., Cifelli, G., Martinello, K., Landolfi, A., Selvetella, G., Grieco, P., Damato, A., et al. (2012). PI3Kγ inhibition reduces blood pressure by a vasorelaxant Akt/L-type calcium channel mechanism. Cardiovasc. Res. *93*, 200–209.

Casagrande, V., Menghini, R., Menini, S., Marino, A., Marchetti, V., Cavalera, M., Fabrizi, M., Hribal, M.L., Pugliese, G., Gentileschi, P., et al. (2012). Overexpression of tissue inhibitor of metalloproteinase 3 in macrophages reduces atherosclerosis in low-density lipoprotein receptor knockout mice. Arterioscler. Thromb. Vasc. Biol. *32*, 74–81.

Chobanian, A.V. (2009). Shattuck Lecture. The hypertension paradox—more uncontrolled disease despite improved therapy. N. Engl. J. Med. *361*, 878–887.

Coffman, T.M. (2011). Under pressure: the search for the essential mechanisms of hypertension. Nat. Med. *17*, 1402–1409.

Crowley, S.D., Gurley, S.B., Oliverio, M.I., Pazmino, A.K., Griffiths, R., Flannery, P.J., Spurney, R.F., Kim, H.S., Smithies, O., Le, T.H., and Coffman, T.M. (2005). Distinct roles for the kidney and systemic tissues in blood pressure regulation by the renin-angiotensin system. J. Clin. Invest. *115*, 1092–1099.

De Falco, S., Gigante, B., and Persico, M.G. (2002). Structure and function of placental growth factor. Trends Cardiovasc. Med. *12*, 241–246.

Dutta, P., Courties, G., Wei, Y., Leuschner, F., Gorbatov, R., Robbins, C.S., Iwamoto, Y., Thompson, B., Carlson, A.L., Heidt, T., et al. (2012). Myocardial infarction accelerates atherosclerosis. Nature *487*, 325–329.

Gigante, B., Morlino, G., Gentile, M.T., Persico, M.G., and De Falco, S. (2006). Plgf-/-eNos-/- mice show defective angiogenesis associated with increased oxidative stress in response to tissue ischemia. FASEB J. *20*, 970–972.

Gurley, S.B., Riquier-Brison, A.D., Schnermann, J., Sparks, M.A., Allen, A.M., Haase, V.H., Snouwaert, J.N., Le, T.H., McDonough, A.A., Koller, B.H., and Coffman, T.M. (2011). AT1A angiotensin receptors in the renal proximal tubule regulate blood pressure. Cell Metab. *13*, 469–475.

Guzik, T.J., Hoch, N.E., Brown, K.A., McCann, L.A., Rahman, A., Dikalov, S., Goronzy, J., Weyand, C., and Harrison, D.G. (2007). Role of the T cell in the genesis of angiotensin II induced hypertension and vascular dysfunction. J. Exp. Med. *204*, 2449–2460.

Harrison, D.G. (2013). The mosaic theory revisited: common molecular mechanisms coordinating diverse organ and cellular events in hypertension. J. Am. Soc. Hypertens. *7*, 68–74.

Harrison, D.G., Vinh, A., Lob, H., and Madhur, M.S. (2010). Role of the adaptive immune system in hypertension. Curr. Opin. Pharmacol. *10*, 203–207.

Ishibashi, M., Hiasa, K., Zhao, Q., Inoue, S., Ohtani, K., Kitamoto, S., Tsuchihashi, M., Sugaya, T., Charo, I.F., Kura, S., et al. (2004). Critical role of monocyte chemoattractant protein-1 receptor CCR2 on monocytes in hypertension-induced vascular inflammation and remodeling. Circ. Res. *94*, 1203–1210.

Kim, S., and Iwao, H. (2000). Molecular and cellular mechanisms of angiotensin II-mediated cardiovascular and renal diseases. Pharmacol. Rev. *52*, 11–34.

King, A.J., Osborn, J.W., and Fink, G.D. (2007). Splanchnic circulation is a critical neural target in angiotensin II salt hypertension in rats. Hypertension *50*, 547–556.

Lawes, C.M., Vander Hoorn, S., and Rodgers, A.; International Society of Hypertension (2008). Global burden of blood-pressure-related disease, 2001. Lancet *371*, 1513–1518.

Li, H., Weatherford, E.T., Davis, D.R., Keen, H.L., Grobe, J.L., Daugherty, A., Cassis, L.A., Allen, A.M., and Sigmund, C.D. (2011). Renal proximal tubule angiotensin AT1A receptors regulate blood pressure. Am. J. Physiol. Regul. Integr. Comp. Physiol. *301*, R1067–R1077.

Loging, W.T., and Reisman, D. (1999). Inhibition of the putative tumor suppressor gene TIMP-3 by tumor-derived p53 mutants and wild type p53. Oncogene *18*, 7608–7615.

Luttun, A., Tjwa, M., Moons, L., Wu, Y., Angelillo-Scherrer, A., Liao, F., Nagy, J.A., Hooper, A., Priller, J., De Klerck, B., et al. (2002). Revascularization of ischemic tissues by PlGF treatment, and inhibition of tumor angiogenesis, arthritis and atherosclerosis by anti-Flt1. Nat. Med. *8*, 831–840.

Madhur, M.S., and Harrison, D.G. (2012). Synapses, signals, CDs, and cytokines: interactions of the autonomic nervous system and immunity in hypertension. Circ. Res. *111*, 1113–1116.

Marvar, P.J., Thabet, S.R., Guzik, T.J., Lob, H.E., McCann, L.A., Weyand, C., Gordon, F.J., and Harrison, D.G. (2010). Central and peripheral mechanisms of T-lymphocyte activation and vascular inflammation produced by angiotensin II-induced hypertension. Circ. Res. *107*, 263–270.

Mueller, S.N., and Germain, R.N. (2009). Stromal cell contributions to the homeostasis and functionality of the immune system. Nat. Rev. Immunol. *9*, 618–629.

Packard, R.R., Lichtman, A.H., and Libby, P. (2009). Innate and adaptive immunity in atherosclerosis. Semin. Immunopathol. *31*, 5–22.

Pan, P., Fu, H., Zhang, L., Huang, H., Luo, F., Wu, W., Guo, Y., and Liu, X. (2010). Angiotensin II upregulates the expression of placental growth factor in human vascular endothelial cells and smooth muscle cells. BMC Cell Biol. *11*, 36.

Perelman, N., Selvaraj, S.K., Batra, S., Luck, L.R., Erdreich-Epstein, A., Coates, T.D., Kalra, V.K., and Malik, P. (2003). Placenta growth factor activates monocytes and correlates with sickle cell disease severity. Blood *102*, 1506–1514.

Pipp, F., Heil, M., Issbrücker, K., Ziegelhoeffer, T., Martin, S., van den Heuvel, J., Weich, H., Fernandez, B., Golomb, G., Carmeliet, P., et al. (2003). VEGFR-1-selective VEGF homologue PlGF is arteriogenic: evidence for a monocyte-mediated mechanism. Circ. Res. *92*, 378–385.

Shao, Q., Ning, H., Lv, J., Liu, Y., Zhao, X., Ren, G., Feng, A., Xie, Q., Sun, J., Song, B., et al. (2012). Regulation of Th1/Th2 polarization by tissue inhibitor of metalloproteinase-3 via modulating dendritic cells. Blood *119*, 4636–4644.

Song, J., Lei, F.T., Xiong, X., and Haque, R. (2008). Intracellular signals of T cell costimulation. Cell. Mol. Immunol. *5*, 239–247.

Steinberg, G., Khankin, E.V., and Karumanchi, S.A. (2009). Angiogenic factors and preeclampsia. Thromb. Res. *123* (*Suppl 2*), S93–S99.

Svendsen, U.G. (1976). Evidence for an initial, thymus independent and a chronic, thymus dependent phase of DOCA and salt hypertension in mice. Acta Pathol. Microbiol. Scand. [A] *84*, 523–528.

Swirski, F.K., Nahrendorf, M., Etzrodt, M., Wildgruber, M., Cortez-Retamozo, V., Panizzi, P., Figueiredo, J.L., Kohler, R.H., Chudnovskiy, A., Waterman, P., et al. (2009). Identification of splenic reservoir monocytes and their deployment to inflammatory sites. Science *325*, 612–616.

Van de Veire, S., Stalmans, I., Heindryckx, F., Oura, H., Tijeras-Raballand, A., Schmidt, T., Loges, S., Albrecht, I., Jonckx, B., Vinckier, S., et al. (2010). Further pharmacological and genetic evidence for the efficacy of PlGF inhibition in cancer and eye disease. Cell *141*, 178–190.

Vaziri, H., Dessain, S.K., Ng Eaton, E., Imai, S.I., Frye, R.A., Pandita, T.K., Guarente, L., and Weinberg, R.A. (2001). hSIR2(SIRT1) functions as an NAD-dependent p53 deacetylase. Cell *107*, 149–159.

Vinh, A., Chen, W., Blinder, Y., Weiss, D., Taylor, W.R., Goronzy, J.J., Weyand, C.M., Harrison, D.G., and Guzik, T.J. (2010). Inhibition and genetic ablation of the B7/CD28 T-cell costimulation axis prevents experimental hypertension. Circulation *122*, 2529–2537.

Wenzel, P., Knorr, M., Kossmann, S., Stratmann, J., Hausding, M., Schuhmacher, S., Karbach, S.H., Schwenk, M., Yogev, N., Schulz, E., et al. (2011). Lysozyme M-positive monocytes mediate angiotensin II-induced arterial hypertension and vascular dysfunction. Circulation *124*, 1370–1381.

Zigmond, R.E., and Ben-Ari, Y. (1977). Electrical stimulation of preganglionic nerve increases tyrosine hydroxylase activity in sympathetic ganglia. Proc. Natl. Acad. Sci. USA *74*, 3078–3080.